

The carbon isotopic composition of atmospheric methane
and its constraint on the global methane budget

John B. Miller

A contribution to the BASIN book.

Draft, Aug. 21, 2002

1. Introduction

Chapter Overview

In this chapter we will develop the context of how the carbon isotopic composition of atmospheric methane can be used to estimate source and sink fluxes. First, we will describe the theory behind using atmospheric measurements to constrain surface sources and sinks and then apply this specifically to isotopic ratios in the atmosphere. Then we will review the history of atmospheric $\delta^{13}\text{C}$ measurements. In the next section we will use these measurements to estimate sources and sinks and examine the sensitivity of our estimates to uncertainties in our model's parameters. We will end with a brief discussion of how other isotopic species like $^{14}\text{CH}_4$ and CH_3D might add to the information contained within the $\delta^{13}\text{C}$ data.

The Importance of CH_4 in the atmosphere.

Atmospheric CH_4 is an important chemical component of both the stratosphere and troposphere and is a major contributor to the enhanced greenhouse effect. In the stratosphere, methane is a major source of water vapor (Jones and Pyle, 1984), and is the primary sink for chlorine radicals (Cicerone and Oremland, 1988), and thus plays an important role in the regulation of stratospheric ozone levels. In the troposphere, CH_4 consumes about 25% of all hydroxyl radicals, and as a result is an *in situ* source of CO and O_3 (Thompson, 1992). Methane strongly absorbs outgoing longwave radiation (OLR) around $7.7\ \mu\text{m}$, a “window” of the earth's emitted infrared spectrum where neither water nor carbon dioxide absorbs strongly. Models indicate that methane's contribution to greenhouse warming is twenty times that of CO_2 on a per molecule basis (Lashof and Ahuja, 1990). It is estimated that methane accounts for approximately 20 % of the increase in radiative forcing by trace gases since the onset of the

industrial era (Lelieveld et al., 1998). Moreover, because the present-day methane budget is close to being in balance, the opportunity exists to actually *reduce* atmospheric CH₄ concentrations by reducing anthropogenic sources, and thus reduce the concentration of an important greenhouse gas (Hansen and Sato, 2001).

The mole fraction of methane in the atmosphere has more than doubled in the last one-hundred-fifty years (Etheridge et al., 1992; Etheridge et al., 1998) and over that time has been highly correlated with human population growth (Blunier et al., 1993). The growth rate of methane in the atmosphere has averaged nearly 1% per year over the last 40 years but has decreased substantially in the last 8 years (Dlugokencky et al., 1998). Neither the rapid increase nor the recent slowdown is clearly understood, and this is directly related to the large uncertainties in the magnitudes and spatial distribution of identified methane sources. Estimates of the magnitudes of various sources have been based upon scaled-up field measurements and forward (Fung et al., 1991) and inverse (Brown, 1993; Hein et al., 1997; Houweling et al., 1999) modeling approaches based on atmospheric measurements. Nonetheless, considerable uncertainties remain in the estimates of source magnitudes.

The methane budget

The top-down approach

Understanding the variability of the CH₄ growth rate is a prerequisite to predicting future atmospheric concentrations. The basic approach in understanding concentrations and trends in concentrations of well-mixed atmospheric gases is to construct a budget for these gases. The budget expresses the imbalance between sources and sinks to the atmosphere, such that the difference between sources and sinks is equal to the growth rate in the atmosphere. If something

is known about atmospheric circulation, spatial patterns in atmospheric concentration can impose significant constraints on the geographic location of sources and sinks (e.g., Tans et al., 1990; Fung et al., 1991). Seasonal variations in concentration are often a direct result of seasonal source and sink activity and are yet another constraint on source and sink activity (Dlugokencky et al., 1997; Randerson et al., 1997). However, with all the ways that concentration data can be analyzed, the budget of CH₄ is still under-constrained.

The bottom-up approach

It is also possible to estimate the sources of CH₄ independent of any atmospheric information. Measurements of CH₄ fluxes made at the local-scale from wetlands, animals or biomass burning can be scaled up in space and time (e.g. Aselmann and Crutzen, 1989; Hao and Ward, 1993). Process-based models of emissions can also be used to estimate fluxes from wetlands (Cao et al., 1996; Walter and Heimann, 2000) and rice paddies (Cao et al., 1995). Economic and fossil fuel production statistics can also be used to estimate fluxes of CH₄ from fossil fuel related activities (Olivier et al., 1999; van Aardenne et al., 2001). On the sink side, OH concentrations can be estimated from CH₃CCl₃ (Prinn et al., 1995; Montzka et al., 2000), and when combined with laboratory based estimates of the rate coefficient of CH₄ + OH (Vaghjiani and Ravishankara, 1991), can be used to estimate the predominant CH₄ sink. Process models have also been used to estimate the magnitude of the soil sink (Ridgwell et al., 1999). Table 1 shows bottom-up estimates of CH₄ sources and sinks based on the work of Lelieveld *et al.* (1998). If the total amount of methane consumed in a year is known well, the sum of all bottom-up estimates can be checked against atmospheric measurements. This is because this sum must

equal the observed annual increase of atmospheric methane (equation 1), which can be measured very accurately.

Isotopic Budgets

Measuring the $^{13}\text{C}:^{12}\text{C}$ ratio of CH_4 allows us to use the temporal and spatial patterns of two molecular species, instead of one, to constrain the global CH_4 budget. However, the budget will not be fully constrained. To do that we would need to add an independently behaving isotopic species for every term in the budget. Nonetheless, the more isotopic species we measure, the more aspects of the budget can be constrained. From the atmospheric (or top-down) perspective, we can describe the global CH_4 budget using equation (1).

$$\frac{d[\text{CH}_4]}{dt} = Q - \frac{[\text{CH}_4]}{\tau} \quad (1)$$

where Q is the sum of all methane sources and τ is the lifetime of CH_4 methane in the atmosphere. Simply put, the accumulation of methane in the atmosphere is equal to the difference in source and sink fluxes. We can measure the methane mole fraction and its rate of change, so if we can estimate τ based on the global mean OH concentration (and minor contributions from consumption in soil and destruction by molecules other than OH), then we can determine the total flux of all methane sources, Q .

Before proceeding we will define δ , the isotopic ratio expressed as per mil (‰) or part per thousand:

$$\delta \equiv \left(\frac{R_{\text{sample}}}{R_{\text{standard}}} - 1 \right) 1000 \text{‰} \quad (2)$$

where R =(rare isotope/abundant isotope). If we can measure the carbon isotopic ratio of methane in the atmosphere, $\delta^{13}\text{C}$, and know the fractionation associated with its destruction by

OH and other processes, then we can estimate the flux weighted mean isotopic ratio of all methane sources, δ_q .

$$\mathbf{d}_q = \mathbf{a} \mathbf{d}_a + \mathbf{e} \quad (3)$$

where δ_a is the isotopic ratio of atmospheric methane and ϵ is the sink-weighted fractionation factor of all sink processes. $\epsilon = (\alpha - 1)1000$, where $\alpha = k_{\text{rare}}/k_{\text{abundant}}$ and k is the rate coefficient for any unidirectional chemical or physical process. Equation 3 is a common approximation that assumes both the methane concentration and isotopic ratio are at steady-state in the atmosphere. Knowing Q and δ_q imposes a constraint on the magnitude of individual methane sources or source-types, *i.e.* those sources with common characteristic isotopic ratios.

In particular, methane sources may be divided into three categories: bacterially produced methane, like that from wetlands or ruminant animals; fossil-fuel methane, like that associated with coal and natural gas deposits; and methane produced from biomass burning. Each of these three classes has a fairly distinct isotopic signature, with bacterial methane $\delta^{13}\text{C} \cong -60\text{‰}$, thermogenic methane $\delta^{13}\text{C} \cong -40\text{‰}$, and biomass burning methane $\delta^{13}\text{C} \cong -25\text{‰}$ (e.g. Quay et al., 1991). Individual methane sources may differ significantly from their source type's characteristic signature (Conny and Currie, 1996), but the average values above are probably valid on large spatial scales.

If we split up all methane sources into bacterial, thermogenic and biomass burning fractions we can write the following equations:

$$Q = Q_{\text{bact}} + Q_{\text{ff}} + Q_{\text{bmb}} \quad (4)$$

$$\mathbf{d}_q Q = \mathbf{d}_{\text{bact}} Q_{\text{bact}} + \mathbf{d}_{\text{ff}} Q_{\text{ff}} + \mathbf{d}_{\text{bmb}} Q_{\text{bmb}} \quad (5)$$

where 'bact' is the bacterial fraction, 'ff' the fossil fuel related, or thermogenic fraction, and 'bmb' the biomass burning fraction. Now we have two equations with three unknowns, so we

cannot uniquely partition Q unless we specify a value for the bacterial, thermogenic or biomass burning fraction. Later, we will use $^{14}\text{CH}_4$ data to specify Q_{ff} and then solve equations 4 and 5. However, even with three unknowns the constraint provided by equations 4 and 5 is powerful, because there is a limited set of source fluxes that will satisfy both equations. This is especially true for the biomass burning fraction, because its source signature of -25‰ differs more from δ_q than the other source signatures. Additionally, any bottom-up estimate of these source fractions must also satisfy equations 4 and 5.

2. d^{13}CH_4 Observations

Measurement techniques

$\delta^{13}\text{C}$ of methane measurements are most often made on air that has been sampled into a low pressure (3-10 psig) flask or high pressure cylinder (500-2000 psig). Traditional analysis methods (e.g. Stevens and Rust, 1982) use 15 – 60 L of air and therefore use air from high pressure or high volume cylinders. In these “off-line” analyses, air is extracted from the cylinder and the CO is converted to CO_2 , which along with the original CO_2 is cryogenically removed from the air sample. After non-methane hydrocarbons are removed, the sample is combusted and the resulting CO_2 is separated from the air cryogenically and analyzed on a dual-inlet isotope ratio mass spectrometer (IRMS) where its isotopic ratio is compared to CO_2 with a known carbon isotopic ratio. Typical precision for the traditional “off-line” $\delta^{13}\text{C}$ analysis is 0.02 – 0.05 ‰, but the process requires a large amount of air and is labor intensive.

In contrast to traditional analyses, a gas chromatography – isotope ratio mass spectrometry (GC-IRMS) system can use about a factor of 10^3 less air (10-50 mL) than the traditional system. In high precision GC-IRMS systems for methane $\delta^{13}\text{C}$ analysis (Rice et al.,

2001; Miller et al., 2002) 10-50 mL of air is entrained in a helium stream and transferred to a -130° C substrate, where methane is retained but air (N₂, O₂, and Ar) is vented. The concentrated CH₄ then passes through a chromatographic column where it is separated from residual air as well as CO and CO₂. The CH₄ peak eluting from the column is then combusted to form CO₂ which enters the mass spectrometer. Its isotopic ratio is calculated by integrating and ratioing the m/e = 44, 45, and 46 peaks arriving at the mass spectrometer collector cups. The precision of GC-IRMS systems ranges from 0.04 – 0.20 ‰, but this sacrifice is small compared to relative sample size requirements, which allows for easier collection of atmospheric samples and shorter analysis times. The GC-IRMS process can also be automated allowing for a much higher throughput of samples compared to the traditional method (Miller et al., 2002).

History of Atmospheric and Surface δ¹³C Measurements

The first sustained atmospheric measurements of δ¹³C of CH₄ were by Stevens (1995), who reported 201 measurements, mostly from assorted sites in the continental United States, between 1978 and 1989. Quay *et al.* (1991; 1999, <http://cdiac.esd.ornl.gov>) reported over 1000 measurements between 1987 and 1996 from bi-weekly sampling at Pt. Barrow, AK (BRW), Olympic Peninsula, WA, and Mauna Loa, HI (MLO), in addition to less frequent sampling at Cape Grim, Tasmania (CGO), Fraserdale, Canada, the Marshal Islands and from Pacific Ocean ship transects. δ¹³C of methane in the Southern Hemisphere has been regularly monitored at Baring Head, New Zealand since 1990 (Lowe et al., 1994), and regular measurements of δ¹³C have also been made at Niwot Ridge, CO (NWR) and Montana de Oro, CA (Gupta et al., 1996; Tyler et al., 1999) since 1989 and 1995, respectively, and Izana, Tennerife since 1997 (Saueressig et al., 2001). More than 2000 measurements of δ¹³C in CH₄ have also been weekly at

six of the NOAA/CMDL Cooperative Air Sampling Network sites since January 1998 (Miller et al., 2002). Currently, $\delta^{13}\text{C}$ of methane is being measured at thirteen of the NOAA/CMDL network sites (see <ftp.cmdl.noaa.gov/ccg/ch4c13>). The total of regularly monitored sites, for which references exist in the literature, is 19.

In addition to measurements of $\delta^{13}\text{C}$ in atmospheric methane, measurements of source isotopic signatures are necessary to apply the isotopic budget approach. Table 1 lists references for measurements of methane source and sink signatures. The large variety of biogeochemical processes that produce methane means that no single model can be used to predict the isotopic signature of methane fluxes. Instead, global estimates of isotopic ratios in methane emissions are based mainly on a relatively small number of field measurements (e.g. Tyler, 1986; Conny and Currie, 1996). Recent progress has been made in better understanding the isotopic signature of emissions from wetlands (e.g. Popp et al., 1999), rice paddies (e.g. Chidthaisong et al., 2002; Kruger et al., 2002) and landfills (e.g. Liptay et al., 1998; Chanton and Liptay, 2000). However, the biogeochemical complexity of the processes, and the lack of measurements of variables thought to influence those processes precludes the use of a predictive model for isotopic signatures at this time. This stands in sharp contrast to the case of CO_2 fractionation, where well-tested models exist that predict the fractionation occurring during assimilation of CO_2 by both C_3 and C_4 plants (e.g. Farquhar et al., 1989).

Firn, Ice Core and air archive measurements

While there have been numerous measurements of the paleo-atmospheric concentration of methane over decadal (Battle et al., 1996), centennial (Nakazawa et al., 1993; Etheridge et al., 1998), and millennial and longer scales (Blunier et al., 1995; Brook et al., 1996; Chappellaz et

al., 1997), there have been only a few measurements of $\delta^{13}\text{C}$ in atmospheric CH_4 made on pre-1978 air. Craig *et al.* (1988) reported two values of $\delta^{13}\text{C}$ from a Northern Hemisphere ice core with a gas age estimated to be about 200 years before present. Sowers recently measured the $\delta^{13}\text{C}$ of methane trapped in Antarctic ice spanning the last glacial/inter-glacial transition (33k-2k yr. before present) (Sowers, 2000b) and from Greenland ice during the pre-industrial period (20–200 yr. before present) (Sowers, 2000a). More recently, Braunlich *et al.* (2001) presented $\delta^{13}\text{C}$ measurements of air trapped in firn as old as 50 years. Francey *et al.* (1999) have also reported a $\delta^{13}\text{C}$ record derived from both Antarctic firn air and air archived in high-pressure cylinders.

Sowers (2000b) found that glacial (e.g. 20 kyr. before present) values of $\delta^{13}\text{C}$ were 3.4 ‰ heavier than average pre-industrial Holocene (12 kyr.-present) values. Over the same time period, methane concentrations increased from about 380 ppb during the last glacial period to 700 ppb in the pre-industrial Holocene (Chappellaz *et al.*, 1990). Sowers attributed these changes to a doubling in methane emissions from northern wetlands following deglaciation. This was based on the idea that the isotopic signature for northern wetland emissions is about –65‰ whereas for tropical emissions it is –53‰ (Stevens, 1993). However, the uncertainty in the isotopic signature of wetlands emissions in one region can be as large as the apparent latitudinal gradient (Conny and Currie, 1996). Using a single value for wetlands emissions of –60‰, these measured changes in CH_4 and $\delta^{13}\text{C}$ following deglaciation can be explained by a doubling of global wetland emissions from 80 to 160 Tg/yr.

For ice core air with a gas age of 200 years before present, Sowers measured a $\delta^{13}\text{C}$ value of –49.2‰ which is similar to that of Craig *et al.* (1988) who measured a value of –49.6‰. The measurements of Craig *et al.* (1988) were not corrected for diffusional fractionation in the firn layer (Francey *et al.*, 1999), which may explain the offset between the two sets of measurements.

Both of these values are significantly heavier than previous model estimates (Miller, 1999; Lassey et al., 2000), and could be evidence that estimates of pre-industrial biomass burning are too low. Firn gas and air archive measurements do match the model estimates very well, but the measurements extend only as far back as 1950. More measurements of $\delta^{13}\text{C}$ from firn and recent ice cores are needed to paint a clearer picture of the pre-industrial and early industrial methane budget.

Modern trend, latitudinal gradient, and seasonal cycles.

20th Century Trend

The firn and air-archive records show that as methane concentration increased during the second half of the 20th century, $\delta^{13}\text{C}$ also increased. While the CH_4 mole fraction increased at a rate of about 10 ppb/yr, $\delta^{13}\text{C}$ increased at about 0.03‰/yr. These increases are most likely a result of the dramatic increase in global fossil fuel use and an increase in biomass burning. These are the only two source classes that could make the value of atmospheric $\delta^{13}\text{C}$ more positive.

Starting in the mid 1980s and continuing on until the end of the century, the globally averaged CH_4 growth rate slowed substantially from 13 ppb/yr in 1985 to about 3 ppb/yr in 1999. Likewise, Francey *et al.* (1999) have shown that the growth rate of $\delta^{13}\text{C}$ also has slowed down, although the slowdown appears to begin in the mid 1990s as opposed to the mid-1980s. What was the cause of the slowdowns in CH_4 and $\delta^{13}\text{C}$? Dlugokencky *et al.* (1998) showed that as long as $\hat{\delta}$ was assumed to be constant over time (Prinn et al., 1995), the source term Q (equation 1) remained nearly constant over this time. The decrease in the growth rate of CH_4 could then be explained best as the approach of the sources and sinks toward steady-state, i.e.

$d[\text{CH}_4]/dt=0$. The analysis by Francey *et al.* (1999) of $\delta^{13}\text{C}$ from the Cape Grim Air Archive also supports the notion that both Q and $\hat{\delta}$ have been nearly constant and that the system is approaching steady-state. That the $\delta^{13}\text{C}$ growth rate slowed down some years after CH_4 is also consistent with the ideas of Tans (1997) who pointed out that the perturbation adjustment time for $\delta^{13}\text{C}$ is longer than that of CH_4 .

Most recently, the growth rates for both CH_4 and $\delta^{13}\text{C}$ have been nearly flat since 1999. Dlugokencky *et al.* (1998) estimated that steady-state for atmospheric CH_4 might be reached in the next twenty years. The current steady-state, however, is more likely a result of the decay of the huge pulse of global methane emissions that occurred during 1998 as a result of increased emissions from northern and tropical wetlands and northern biomass burning (Dlugokencky *et al.*, 2001).

Latitudinal Gradient

The north-south gradients in methane mole fraction and its isotopic composition are important constraints on the location and strength of methane sources and sinks (Fung *et al.*, 1991). The mole fraction latitudinal gradient is well established (e.g. Steele *et al.*, 1987; Dlugokencky *et al.*, 1994), and Quay *et al.* (1991; 1999) and Miller *et al.* (2002) have reported an annual mean gradient for $\delta^{13}\text{C}$. Figure 1 shows the annual mean gradients for 1998-2000 between 90°S and 71°N . The average difference between South Pole (SPO) and Barrow, AK, (BRW – SPO) was $-0.65 \pm 0.1\text{‰}$ in 1998, $-0.48 \pm 0.1\text{‰}$ in 1999 and $-0.48 \pm 0.1\text{‰}$ in 2000. Quay *et al.* (1991) reported a mean annual average difference of $-0.54 \pm 0.05\text{‰}$ between BRW (71°N) and CGO (41°S) during the years 1989 - 1995. For the period 1998-2000 the mean hemispheric difference from the six sites in Figure 1 is 0.19‰ . It is important to note that two of

the Northern Hemisphere sites, MLO and NWR are both situated at altitudes greater than 3000m. We know that the methane mole fraction at these sites is substantially less than at sites at comparable latitudes but at sea level. It is likely that the Northern Hemisphere average $\delta^{13}\text{C}$ calculated here is too positive, because we know that $\delta^{13}\text{C}$ values increase with height (Tyler et al., 1999). Thus, it is also likely that we have underestimated the inter-hemispheric difference. For the purposes of the model (see below) we have attempted to correct for these altitude effects, which the values in Table 2 reflect.

The $\delta^{13}\text{C}$ values in the Southern Hemisphere are higher than $\delta^{13}\text{C}$ values in the Northern Hemisphere. This feature is the combined effect of two separate processes. The majority of emissions originate in the Northern Hemisphere, and the reaction with OH enriches the ^{13}C content of the methane remaining in the atmosphere. Methane reaching the Southern Hemisphere has had more time to react with OH than methane in the Northern Hemisphere, leaving it more enriched in ^{13}C . Another prominent feature is the lack of a significant $\delta^{13}\text{C}$ gradient in the Southern Hemisphere, which can be explained by low emissions and rapid atmospheric mixing (Law et al., 1992).

Southern Hemisphere Seasonal cycles

Southern Hemisphere sites SPO (90° S), CGO (41° S), and SMO (14° S) do not exhibit strong seasonal variability in the NOAA/CMDL data set, except during 1998 (Figure 2). During this period substantial decreases in $\delta^{13}\text{C}$ values are present during August, September and October, especially at SMO and CGO. The conventional assumption is that seasonal variations in SH mole fractions are driven mostly by OH oxidation, but the magnitude of the dip in $\delta^{13}\text{C}$ values is too large to be explained by OH alone. One possible contribution to the observed dip is

the positive 12 Tg/yr anomaly in tropical wetland emissions during 1998 proposed by *Dlugokencky et al.* (2001). A +12 Tg/yr anomaly would result in a -0.13‰ anomaly in the lower Southern atmosphere (0-30°S) if the emissions mixed evenly through the entire semi-hemisphere and if the signature of the wetland source were -60‰. The seasonal cycle amplitudes at CGO, based on the smooth curve fit to the data (Miller et al., 2002), were 0.30‰ in 1998, 0.17‰ in 1999, and 0.15‰ in 2000. Large tropical wetland emission could help to explain the presence of the dip at SMO and CGO in 1998.

Lowe *et al.* (1997) showed distinct seasonal cycles in $\delta^{13}\text{C}$ between 1989 and 1997 from air collected at Baring Head. They calculated that the amplitude of the observed seasonal cycle was too large to be explained solely on the basis of OH oxidation. If the methane mole fraction seasonal amplitude were controlled completely by OH destruction (as might be the case at the South Pole), the amplitude of the $\delta^{13}\text{C}$ signal would be at most 0.1 ‰ according to the following Rayleigh model of CH_4 consumption.

$$d - d_o \approx -\epsilon \frac{\Delta M}{M} \quad (6)$$

Here, δ and δ_o are the original, and final isotopic ratios, expressed in δ -notation (‰ units), ϵ is the kinetic fraction factor due to reaction with OH ($\epsilon = -5.4\text{‰}$ (Cantrell et al., 1990) or $\epsilon = -3.9\text{‰}$ (Saueressig et al., 2001)) and $\Delta M/M$ is the fraction of total methane destroyed ($\Delta M/M = 30 \text{ ppb}/1700 \text{ ppb}$ for Southern Hemisphere sites). The expected amplitude is 0.10‰ (-5.4) or 0.07‰ (-3.9). When the seasonal cycles amplitude exceeds these limits, it is an indication that processes other than destruction by OH are at work.

Northern Hemisphere Seasonal cycles

Seasonal variations of $\delta^{13}\text{C}$ are more pronounced in the Northern Hemisphere, because about 75% of methane emissions originate there (Fung et al., 1991). Mean NH mole fractions average about 90 ppb higher than in the Southern Hemisphere, and in 1998-2000 $\delta^{13}\text{C}$ values were about 0.3‰ lower in the NH than in the SH. Seasonal variations are most evident at BRW where the seasonal cycle amplitude has averaged about 0.6‰, with the maximum in May and the minimum at the end of September. The timing of the minimum and maximum indicates high northern sources as the primary driver of seasonal variability. $\delta^{13}\text{C}$ values start to decrease in May and continue through the summer despite the fact that destruction of CH_4 by OH is largest during this time of year. This probably occurs because emissions from isotopically light sources like wetlands are greatest during the summer, and bacterial emissions have 2-3 times the impact on $\delta^{13}\text{C}$ values than OH for the same change in mole fraction. Seasonal patterns at NWR and MLO are less pronounced than at BRW, but like the SH exhibit deeper minima in 1998 (Figure 2).

Calculating CH_4 sources with the help of $\delta^{13}\text{C}$

Global means

Using equation 1 and a value of CH_4 lifetime, $\hat{\delta} = 9.4$ yr, $[\text{CH}_4] = 1750$ ppb, $d[\text{CH}_4]/dt = 5$ ppb/yr, and a conversion factor of 2.767 ppb/Tg (Fung et al., 1991), we find that $Q = 529$ Tg/yr. Using the exact formulation of Lassey *et al.* (2000), we will calculate δ_q :

$$\mathbf{d}_q = \mathbf{a}\mathbf{d}_a + \mathbf{e} - \frac{\mathbf{e}(1 + \mathbf{d}_a/1000)}{Q} \frac{d[\text{CH}_4]}{dt} + \frac{d\mathbf{d}_a}{dt} \frac{[\text{CH}_4]}{Q} \quad (7)$$

Using a global mean value of $\delta_a = -47.1$ ‰, a value of $\epsilon = -6.3$ ‰, and a $\delta^{13}\text{C}$ growth rate of 0.01‰/yr , we find that the global, flux weighted isotopic signature of all source, $\delta_q = -53.2$ ‰. Now we can use equations 4, and 5 to estimate the annual global CH_4 emissions from bacterial processes and biomass burning after separately calculating fossil fuel emissions using $^{14}\text{CH}_4$ data. Based on the data of Quay *et al.* (1999) we find the fossil fuel related flux of CH_4 to be 100 Tg/yr. Assuming values for δ_{ff} , δ_{bmb} , and δ_{bio} of -40, -25, and -60 ‰, the global value of $Q_{\text{bmb}} = 46$ Tg/yr and $Q_{\text{bio}} = 383$ Tg/yr. This simple calculation produces estimates of Q_{bmb} and Q_{bio} that are similar to those in Table 1, where $Q_{\text{bio}}=420$ Tg/yr and $Q_{\text{bmb}}=40$ Tg/yr.

Results from an inverse 2-box model

The spatial patterns in the $\delta^{13}\text{C}$ and CH_4 data, specifically the latitudinal gradient, can be used to infer the spatial distribution of CH_4 sources. In the following example, we use a two-box model of the atmosphere, and therefore use the inter-hemispheric difference. We again specify the fossil fuel flux based on $^{14}\text{CH}_4$ data but now include emissions from landfills because of their similar spatial patterns. Dividing the Earth at the equator, we can solve for the emissions from bacterial processes and biomass burning in each hemisphere, if we know the inter-hemispheric exchange constant, k_{ex} . In equations 8 –11 we have four equations and four unknowns: bacterial and biomass burning emissions for the Northern and Southern Hemispheres. The values of all the other terms are listed in Table 2.

$$\dot{X}_N = B_N + BMB_N + FFP_N + k_{12}X_N + k_{\text{ex}}(X_N - X_S) \quad (8)$$

$$\dot{X}_S = B_S + BMB_S + FFP_S + k_{12}X_S - k_{\text{ex}}(X_N - X_S) \quad (9)$$

$$\dot{d}_N = \frac{B_N}{X_N}(d_B - d_N) + \frac{BMB_N}{X_N}(d_{BMB} - d_N) + \frac{FFP_N}{X_N}(d_{FFP} - d_N) + \epsilon k_{12} + k_{\text{ex}} \frac{X_S}{X_N}(d_N - d_S) \quad (10)$$

$$\dot{\mathbf{d}}_S = \frac{B_S}{X_S}(\mathbf{d}_B - \mathbf{d}_S) + \frac{BMB_N}{X_N}(\mathbf{d}_{BMB} - \mathbf{d}_S) + \frac{FFP_S}{X_S}(\mathbf{d}_{FFP} - \mathbf{d}_S) + \mathbf{e}k_{12} - k_{ex} \frac{X_N}{X_S}(\mathbf{d}_N - \mathbf{d}_S) \quad (11)$$

Here, X represents the mole fraction and the over-dot denotes the time derivative. B is the hemispheric total of bacterial emissions, BMB of biomass burning emissions, and FFP of fossil fuel related emissions, plus those from landfills. Fossil fuel and landfill sources were grouped together because both are estimated to be more than 90% in the Northern Hemisphere.

When we solve these two systems of two linear equations using the best estimates of the terms on the left-hand-side, the global emission totals are: bacterial = 355 ± 48 Tg/yr, biomass burning = 56 ± 37 Tg/yr. The hemispheric totals are $B_N=250 \pm 33$ Tg/yr, $B_S=106 \pm 21$ Tg/yr, $BMB_N=23 \pm 30$ Tg/yr and $BMB_S=31 \pm 10$ Tg/yr. The global ratio of the B , FFP , and BMB emissions is 65/25/10, which is similar that obtained by *Fung et al.* (1991) of 64/25/11, *Crutzen et al.* (1995) of 72/22/6, *Hein et al.* (1997) of 70/22/7, and *Lelieveld et al.* (1998) of 73/19/7.

Uncertainties and Sensitivities

Even though we use a simple two-box model of the atmosphere, this can be an excellent tool to investigate sensitivity of source partitioning to uncertainty in the parameters listed in Table 2. A Monte Carlo approach is used in which all parameters are assigned uncertainties listed in Table 2. To estimate the error, each known term in equations 8 – 11 is represented by a normally distributed set of points such that the mean and standard deviation are equal to the mean and uncertainty in Table 2. Equations 8 – 11 are solved 10,000 times, each time randomly choosing values from the distribution of each term. The uncertainties on the fluxes are then simply the mean and standard deviation of the solutions from the 10,000 trials.

Table 3 lists the calculated sensitivities of the calculated fluxes to the parameters listed in Table 2. The dominant source of uncertainty is the fossil fuel emission rate, especially for

Northern Hemisphere sources. Uncertainty in source δ values is the next most important source of error. The derived fluxes are much less sensitive to the isotopic signature of biomass-burning fluxes than to changes in the signatures of FFP or bacterial emissions. For any source, a 2 per mil change in source signature corresponds to about a 5% change in the flux of that source. 5% of the biomass-burning source is only about 3 Tg, whereas for bacterial emissions 5% is 18 Tg. Global flux partitioning is therefore not terribly sensitive to the isotopic signature of biomass burning emissions but is to the weighted signature of all bacterial emissions. The inter-hemispheric exchange constant, k_{ex} , does not influence global partitioning, but has a big impact on partitioning of a source between hemispheres. For example, although our global BMB value agrees with the earlier estimate of Fung *et al.* (1991), our BMB_S estimate is much different. However, the level of agreement in North/South partitioning is largely a function of our choice of k_{ex} , which is a poorly constrained parameter (Denning *et al.*, 1999).

Interestingly, it is evident that improving the precision and accuracy of our atmospheric measurements will not dramatically alter our ability to partition sources, at least when using annual hemispheric average $\delta^{13}\text{C}$ values. Changing the global average δ by 0.1‰ would only alter emissions partitioning by about 1.5 Tg/yr in our model. The biggest improvements in emission partitioning will come from better constraining fossil fuel emissions and by better understanding the isotopic ratio of bacterial emissions and how and why they vary. Recent measurements of ϵ_{OH} (Saueressig *et al.*, 2001) show a value of -3.9‰, contrasting with the earlier measurement of -5.4‰ (Cantrell *et al.*, 1990). Using the newer value of ϵ_{OH} results in an increase in calculated biomass burning emissions of about 25 Tg with a concomitant decrease in bacterial emissions. The other important way we can improve the sink side of the equation is by

better determining the lifetime of CH₄ in the atmosphere, including the magnitude of the soil sink, and the possible existence of a tropospheric Cl sink.

A role for chlorine?

What is the extent to which atomic Cl in the marine boundary layer (MBL) consumes CH₄? Several recent studies have suggested the possibility that CH₄ is oxidized by Cl in the marine boundary layer (Gupta et al., 1996; Vogt et al., 1996; Wingenter et al., 1999; Allan et al., 2001a; Allan et al., 2001b). Wingenter *et al.* (1999) estimated that 2% of CH₄ in the MBL is destroyed by Cl, but Singh *et al.* (1996) estimated that no more than 2% of CH₄ is consumed by Cl in the troposphere. Because of the large isotopic fractionation the reaction CH₄ + Cl (Saueressig et al., 1995), atmospheric δ¹³C is a good tracer for the activity of Cl. A model experiment (Miller et al., 2002) suggests an upper limit for Cl of 6 % of the total sink. If it were more, the biomass-burning source would be less than 20 Tg/yr, which is unlikely from a bottom-up point of view. However, the absence of a chlorine sink is also consistent with the data.

Three-dimensional Inverse models

The paucity of atmospheric δ¹³C data has limited its inclusion as input into global inverse models studying the CH₄ budget. The inverse model of Hein *et al.* (1997) included a small amount of δ¹³C data. Perhaps not surprisingly, it found that including δ¹³C data did not significantly change the fluxes that were derived solely from CH₄ mole fraction measurements. In this study, δ¹³C measurements from just three Northern Hemisphere sites were used as constraints. As more measurements become available it is likely that δ¹³C measurements will prove more useful as formal constraints in inverse studies.

How can we improve the utility of $\delta^{13}\text{C}$ measurements?

As we have seen above, CH_4 concentration and $\delta^{13}\text{C}$ measurements alone cannot uniquely specify methane sources, even when divided into just three broad categories. To arrive at a unique solution, we added information on the fossil-fuel fraction that was derived from $^{14}\text{CH}_4$ measurements. More generally, $\delta^{13}\text{C}$ measurements will be most useful when measurements of another methane species are added to the mix. Both $^{14}\text{CH}_4$ and CH_3D can serve this role. Measurements of $^{14}\text{CH}_4$ have specific use in determining fossil fuel related emissions. Although this is, in principle, a very powerful tracer, there is considerable uncertainty in the $^{14}\text{CH}_4$ budget related to emissions of $^{14}\text{CH}_4$ from nuclear power plants (Kunz, 1985). The signal of δD in CH_4 may be a strong marker for the latitudinal origin of methane fluxes (Waldron et al., 1999). This is because the source of the hydrogen atoms in bacterially produced methane is water, and there is a strong gradient of δD in H_2O of about 100‰ from equator to pole (Dansgaard, 1964). More importantly, the large difference in CH_3D wetland emissions has also been directly observed (Bellisario et al., 1999; Smith et al., 2000). With the advent of continuous flow measurement techniques for δD of CH_4 (Hilkert et al., 1999; Rice et al., 2001), atmospheric and source δD measurements should become an important complement to the ongoing measurements of $\delta^{13}\text{C}$. As we have seen above in the case of $\delta^{13}\text{C}$, it will be very important to accurately characterize the deuterium signature of CH_4 emissions. Atmospheric $\delta^{13}\text{C}$ measurements, and more generally, isotopic measurements will certainly help us to better understand the global methane budget, but we will need to better understand the processes responsible for determining fractionation during both production and consumption of methane.

Up to this point, the full extent of spatial and temporal information contained within the $\delta^{13}\text{C}$ measurements has not been fully utilized. This will require the merging of data sets between different laboratories using different sample collection, analysis and standardization procedures. Arriving at a unified data set of atmospheric $\delta^{13}\text{C}$ measurements will require common isotopic standards and careful inter-comparison of both sample and reference gases. So, it remains to be seen how much atmospheric $\delta^{13}\text{C}$ measurements will improve our estimates of sources and sinks compared to estimates based on CH_4 alone.

Table 1. Estimates of emission strength and isotopic signature for most sources and sinks grouped by estimated $\delta^{13}\text{C}$ signature

Source	Strength ¹ (Tg/yr)	$\delta^{13}\text{C}$ (‰)	References
Wetlands ²	150	-60 ³	(Quay et al., 1988; Stevens, 1993)
Rice	80	-64 ⁴	(Stevens, 1993; Tyler et al., 1994)
Ruminants	85	-60 ⁵	(Stevens, 1993)
Termites	20	-57	(Tyler, 1986; Gupta et al., 1996)
Landfills	40	-52 ⁶	(Tyler, 1986; Levin et al., 1993)
Wastewater	25	-54 ⁶	(Levin et al., 1999; Lowry et al., 2001)
Animal Waste	30	-52	(Tyler, 1986)
Ocean flux ⁷	10	-43 ⁶	(Holmes et al., 2000; Sansone et al., 2001)
Gas and Coal	110	-40 ⁸	(Deines, 1980; Schoell, 1980)
Biomass burning	40	-25 ⁹	(Craig et al., 1988)
Total/weighted average	590	-52.9	
Sink			
Tropospheric OH ¹⁰	506	-5.4/-3.9 ¹¹	(Cantrell et al., 1990; Saueressig et al., 2001)
Soils	30	-21	(King et al., 1989)
Stratosphere	40	-12 ¹²	(Hein et al., 1997)
Total/weighted average	576	-6.7/-5.4	

Notes:

1. Source strengths based on Lelieveld, 1998
2. Includes Tundra and Freshwater sources
3. Unweighted averages from both review studies
4. 10‰ seasonal cycle in Tyler, 1994
5. Average of C3 and C4 diets
6. Average of two studies
7. Hydrates implicitly included
8. Unweighted average of coal and gas δ values
9. Likely to reflect $\delta^{13}\text{C}$ of plant biomass (C₃ or C₄)
10. From IPCC 2001
11. Fractionation estimates are statistically different at 95%
12. Weighted fractionation of Cl, OH, and O1D

Table 2. Input parameters for two-box model.

	X^a	X^a	δ^b	δ^a	k_{ex}	k_{12}^c	ϵ^d	FFP ^e	δ_B^f	δ_{BMB}^f	δ_{FFP}^f
units	(ppb/yr)	(ppb)	(‰/yr)	(‰)	(1/yr)	(1/yr)	(‰)	(Tg/yr)	(‰)	(‰)	(‰)
N	5.5	1791	0.02 ± 0.02	-47.2	1.0 ± 0.1	0.1071 ± 0.01	-6.4 ± 0.8	124 ± 47	-61 ± 2	-24 ± 2	-43 ± 2
S	10.0	1705	0.02 ± 0.02	-46.9	1.0 ± 0.1	0.1057 ± 0.01	-6.2 ± 0.8	11 ± 4	-61 ± 2	-24 ± 2	-43 ± 2

a. Average of measured values from NOAA/CMDL global network during 1998 - 1999.

b. From Quay *et al.* [1999]

c. Calculated as $k_{12}=k_{OH} + k_{SOIL} + k_{STRAT}$. k_{OH} is 1/10.5 and is taken from Montzka *et al.* [2000]; k_{SOIL} was 1/484.2 and was calculated as a first-order loss assuming a 30 Tg/yr soil sink and a global CH₄ burden of 1750 ppb. We assume that 2/3 of the soil sink is in the Northern Hemisphere. k_{STRAT} is 1/110 and is taken from Scientific Assessment of Ozone Depletion: 1998.

d. $\epsilon=1000(\alpha-1)$. Calculated as $\alpha=(\alpha_{OH}k_{OH} + \alpha_{SOIL}k_{SOIL} + \alpha_{STRAT}k_{STRAT})/k_{12}$. α_{OH} is 0.9946 and is taken from Cantrell *et al.* [1990]; α_{SOIL} is 0.979 and is taken from King *et al.* [1999]; α_{STRAT} is 0.988 and was calculated by weighting α_{OH} and α_{Cl} by the strengths of Cl and OH sinks in the stratosphere according to Hein *et al.* [1997]. Errors were determined only by propagating errors in k_{12} and assigning an error to α_{OH} of 0.0009, the error estimate of Cantrell *et al.* [1990].

e. FFP is the sum of the Fung *et al.* [1991] categories: gas venting, gas leaks, coal mining, and landfills. The total of the fossil fuel categories was 100 Tg/yr and was calculated from Quay *et al.* [1999] ¹⁴CH₄ data. Landfill emissions are taken as 35 Tg/yr, which is the average of the Hein *et al.* [1997] and Fung *et al.* [1991] estimates. The north/south division (92%/8%) is based on Table 4 of Fung *et al.* [1991]. The error estimates are derived from the range in landfill emission estimates (20 Tg/yr) and the range for fossil fuel emissions of 50% given in Quay *et al.* [1999].

f. B (Bacterial emissions) are defined as the sum of the Fung *et al.* categories: bogs, swamps, tundra, rice, animals, termites and clathrates; BMB is biomass burning; FFP defined as above. δ values were calculated using source signatures from Table 1 of Quay *et al.* [1999] with weightings from the global totals of the Fung *et al.* categories listed above. We assume that source signatures are the same for each hemisphere.

Table 3. Sensitivity of source partitioning to parameter changes in the inverse box-model.

Parameter	Units	Source	Sensitivity			Total Uncertainty (Tg) ^a
			Globally	NH	SH	
$\delta_N - \delta_S$	Tg % ⁻¹	B	0	69	-69	0
$X_N - X_S$	Tg ppb ⁻¹	B	0	0.91	-0.91	0
%Cl added	Tg % ⁻¹	B	11.2	3.9	7.3	not estimated
		BMB ^a	-6.3	-2.2	-4.1	not estimated
δ_B	Tg % ⁻¹	B	9.7	7.3	2.4	19.4
δ_{BMB}	Tg % ⁻¹	B	1.5	0.95	0.55	3.0
δ_{FFP}	Tg % ⁻¹	B	6.7	6.3	0.4	13.4
FFP	Tg Tg ⁻¹	B	-0.51	-0.47	-0.04	26.0
d δ /dt	Tg % ⁻¹ yr	B	131	-67	-64	2.6
dX/dt	Tg ppb ⁻¹ yr	B	1.7	0.9	0.8	3.4

a. These are global values computed by multiplying the sensitivity by the estimated uncertainty from Table 2. The uncertainty for dX/dt is set at 2 ppb/yr.

b. For all other source sensitivities, BMB (biomass burning) is simply of the opposite sign as B (bacterial), such that total global emissions remain constant. Adding a Cl sink increases the total emissions in the model, which requires that BMB and B sensitivities not be of equal magnitude.

References:

- Allan, W., Lowe, D. C. and Caine, J. M. 2001a. Active chlorine in the remote marine boundary layer: Modeling anomalous measurements of delta C-13 in methane. *Geophys. Res. Lett.*, **28**, 3239-3242.
- Allan, W., Manning, M. R., Lassey, K. R., Lowe, D. C. and Gomez, A. J. 2001b. Modeling the variation of delta C-13 in atmospheric methane: Phase ellipses and the kinetic isotope effect. *Global Biogeochem. Cycles*, **15**, 467-481.
- Aselmann, I. and Crutzen, P. J. 1989. Global distribution of natural freshwater wetlands and rice paddies, their net primary productivity, seasonality and possible methane sources. *J. Atmos. Chem.*, **8**, 307-358.
- Battle, M., Bender, M., Sowers, T., Tans, P. P., Butler, J. H., Elkins, J. W., Ellis, J. T., Conway, T., Zhang, N., Lang, P. and Clarke, A. D. 1996. Atmospheric gas concentrations over the past century measured in air from firn at the South Pole. *Nature*, **383**, 231-235.
- Bellisario, L. M., Bubier, J. L., Moore, T. R. and Chanton, J. P. 1999. Controls on CH₄ emissions from a northern peatland. *Global Biogeochem. Cycles*, **13**, 81-91.
- Blunier, T., Chappellaz, J., Schwander, J., Stauffer, B. and Raynaud, D. 1995. Variations in Atmospheric Methane Concentration During the Holocene Epoch. *Nature*, **374**, 46-49.
- Blunier, T., Chappellaz, J. A., Schwander, J., Barnola, J. M., Desperets, T., Stauffer, B. and Raynaud, D. 1993. Atmospheric Methane, Record From a Greenland Ice Core Over the Last 1000 Year. *Geophys. Res. Lett.*, **20**, 2219-2222.

- Braunlich, M., Aballanin, O., Marik, T., Jockel, P., Brenninkmeijer, C. A. M., Chappellaz, J., Barnola, J. M., Mulvaney, R. and Sturges, W. T. 2001. Changes in the global atmospheric methane budget over the last decades inferred from C-13 and D isotopic analysis of Antarctic firm air. *J. Geophys. Res.*, **106**, 20465-20481.
- Brook, E. J., Sowers, T. and Orchardo, J. 1996. Rapid variations in atmospheric methane concentration during the past 110,000 years. *Science*, **273**, 1087-1091.
- Brown, M. 1993. Deduction of Emissions of Source Gases Using an Objective Inversion Algorithm and a Chemical-Transport Model. *J. Geophys. Res.*, **98**, 12639-12660.
- Cantrell, C. A., Shetter, R. E., McDaniel, A. H., Calvert, J. G., Davidson, J. A., Lowe, D. C., Tyler, S. C., Cicerone, R. J. and Greenberg, J. P. 1990. Carbon Kinetic Isotope Effect in the Oxidation of Methane By the Hydroxyl Radical. *J. Geophys. Res.*, **95**, 22455-22462.
- Cao, M. K., Dent, J. B. and Heal, O. W. 1995. Modeling Methane Emissions from Rice Paddies. *Global Biogeochem. Cycles*, **9**, 183-195.
- Cao, M. K., Marshall, S. and Gregson, K. 1996. Global carbon exchange and methane emissions from natural wetlands: Application of a process-based model. *J. Geophys. Res.*, **101**, 14399-14414.
- Chanton, J. and Liptay, K. 2000. Seasonal variation in methane oxidation in a landfill cover soil as determined by an in situ stable isotope technique. *Global Biogeochem. Cycles*, **14**, 51-60.
- Chappellaz, J., Barnola, J. M., Raynaud, D., Korotkevich, Y. S. and Lorius, C. 1990. Ice-Core Record of Atmospheric Methane Over the Past 160,000 Years. *Nature*, **345**, 127-131.

- Chappellaz, J., Blunier, T., Kints, S., Dallenbach, A., Barnola, J. M., Schwander, J., Raynaud, D. and Stauffer, B. 1997. Changes in the atmospheric CH₄ gradient between Greenland and Antarctica during the Holocene. *J. Geophys. Res.*, **102**, 15987-15997.
- Chidthaisong, A., Chin, K. J., Valentine, D. L. and Tyler, S. C. 2002. A comparison of isotope fractionation of carbon and hydrogen from paddy field rice roots and soil bacterial enrichments during CO₂/H₂ methanogenesis. *Geochim. Cosmochim. Acta*, **66**, 983-995.
- Cicerone, R. J. and Oremland, R. S. 1988. Biogeochemical aspects of atmospheric methane. *Global Biogeochem. Cycles*, **2**, 299-327.
- Conny, J. M. and Currie, L. A. 1996. The isotopic characterization of methane, non-methane hydrocarbons and formaldehyde in the troposphere. *Atmospheric Environment*, **30**, 621-638.
- Craig, H., Chou, C. C., Welhan, J. A., Stevens, C. M. and Engelkemeir, A. 1988. The Isotopic Composition of Methane in Polar Ice Cores. *Science*, **242**, 1535-1539.
- Crutzen, P. J. 1995 In *Ruminant Physiology: Digestion, metabolism, growth and reproduction: Proceedings of the eighth international symposium on ruminant physiology* (Eds., Engelhardt, W. v., Leonhardt-Marek, S., Breves, G. and Giesecke, D.) Ferdinand Enke Verlag, 291-315.
- Dansgaard, W. 1964. Stable isotopes in precipitation. *Tellus*, **16**, 436-468.
- Deines, P. 1980 In *Handbook of Environmental Isotope Geochemistry*, Vol. 1 (Eds., Fritz, P. and Fontes, J. C.) Elsevier Scientific, 329-406.

- Denning, A. S., Holzer, M., Gurney, K. R., Heimann, M., Law, R. M., Rayner, P. J., Fung, I. Y., Fan, S. M., Taguchi, S., Friedlingstein, P., Balkanski, Y., Taylor, J., Maiss, M. and Levin, I. 1999. Three-dimensional transport and concentration of SF₆ - A model intercomparison study (TransCom 2). *Tellus, Ser. B*, **51**, 266-297.
- Dlugokencky, E. J., Masarie, K. A., Lang, P. M. and Tans, P. P. 1998. Continuing decline in the growth rate of the atmospheric methane burden. *Nature*, **393**, 447-450.
- Dlugokencky, E. J., Masarie, K. A., Tans, P. P., Conway, T. J. and Xiong, X. 1997. Is the amplitude of the methane seasonal cycle changing? *Atmospheric Environment*, **31**, 21-26.
- Dlugokencky, E. J., Steele, L. P., Lang, P. M. and Masarie, K. A. 1994. The Growth-Rate and Distribution of Atmospheric Methane. *J. Geophys. Res.*, **99**, 17021-17043.
- Dlugokencky, E. J., Walter, B. P. and Kaischke, E. S. 2001. Measurements of an anomalous global methane increase during 1998. *Geophys. Res. Lett.*, **28**, 499-503.
- Etheridge, D. M., Pearman, G. I. and Fraser, P. J. 1992. Changes in Tropospheric Methane Between 1841 and 1978 From a High Accumulation-Rate Antarctic Ice Core. *Tellus, Ser. B*, **44**, 282-294.
- Etheridge, D. M., Steele, L. P., Francey, R. J. and Langenfelds, R. L. 1998. Atmospheric methane between 1000 AD and present: Evidence of anthropogenic emissions and climatic variability. *J. Geophys. Res.*, **103**, 15979-15993.
- Farquhar, G. D., Ehleringer, J. R. and Hubick, K. T. 1989. Carbon Isotope Discrimination During Photosynthesis. *Annual Review of Plant Physiology and Plant Molecular Biology*, **9**, 121-137.

- Francey, R. J., Manning, M. R., Allison, C. E., Coram, S. A., Etheridge, D. M., Langenfelds, R. L., Lowe, D. C. and Steele, L. P. 1999. A history of delta C-13 in atmospheric CH₄ from the Cape Grim air archive and antarctic firn air. *J. Geophys. Res.*, **104**, 23631-23643.
- Fung, I., John, J., Lerner, J., Matthews, E., Prather, M., Steele, L. P. and Fraser, P. J. 1991. 3-Dimensional Model Synthesis of the Global Methane Cycle. *J. Geophys. Res.*, **96**, 13033-13065.
- Gupta, M., Tyler, S. and Cicerone, R. 1996. Modeling atmospheric $\delta^{13}\text{C}_{\text{CH}_4}$ and the causes of recent changes in atmospheric CH₄ amounts. *J. Geophys. Res.*, **101**, 22,923-22,932.
- Hansen, J. E. and Sato, M. 2001. Trends of measured climate forcing agents. *PNAS*, **98**, 14778-14783.
- Hao, W. M. and Ward, D. E. 1993. Methane Production from Global Biomass Burning. *J. Geophys. Res.*, **98**, 20657-20661.
- Hein, R., Crutzen, P. J. and Heimann, M. 1997. An inverse modeling approach to investigate the global atmospheric methane cycle. *Global Biogeochem. Cycles*, **11**, 43-76.
- Hilkert, A. W., Douthitt, C. B., Schluter, H. J. and Brand, W. A. 1999. Isotope ratio monitoring gas chromatography mass spectrometry of D/H by high temperature conversion isotope ratio mass spectrometry. *Rapid Comm. Mass. Spec.*, **13**, 1226-1230.

- Holmes, M. E., Sansone, F. J., Rust, T. M. and Popp, B. N. 2000. Methane production, consumption, and air-sea exchange in the open ocean: An evaluation based on carbon isotopic ratios. *Global Biogeochem. Cycles*, **14**, 1-10.
- Houweling, S., Kaminski, T., Dentener, F., Lelieveld, J. and Heimann, M. 1999. Inverse modeling of methane sources and sinks using the adjoint of a global transport model. *J. Geophys. Res.*, **104**, 26,173-26,160.
- Jones, R. L. and Pyle, J. A. 1984. Observations of CH₄ and N₂O by the Nimbus-7 SAMS: a comparison with in situ data and two-dimensional numerical model calculations. *J. Geophys. Res.*, **89**, 5263-5279.
- King, S. L., Quay, P. D. and Lansdown, J. M. 1989. The C-13/C-12 Kinetic Isotope Effect For Soil Oxidation of Methane At Ambient Atmospheric Concentrations. *J. Geophys. Res.*, **94**, 18273-18277.
- Kruger, M., Eller, G., Conrad, R. and Frenzel, P. 2002. Seasonal variation in pathways of CH₄ production and in CH₄ oxidation in rice fields determined by stable carbon isotopes and specific inhibitors. *Global Change Biology*, **8**, 265-280.
- Kunz, C. 1985. Carbon-14 discharge at three light water reactors. *Health Phys.*, **49**, 25-35.
- Lashof, D. A. and Ahuja, D. R. 1990. Relative Contributions of Greenhouse Gas Emissions to Global Warming. *Nature*, **344**, 529-531.
- Lassey, K. R., Lowe, D. C. and Manning, M. R. 2000. The trend in atmospheric methane delta C-13 implications for isotopic constraints on the global methane budget. *Global Biogeochem. Cycles*, **14**, 41-49.

- Law, R., Simmonds, I. and Budd, W. F. 1992. Application of an Atmospheric Tracer Model to High Southern Latitudes. *Tellus*, **44**, 358-370.
- Lelieveld, J., Crutzen, P. J. and Dentener, F. J. 1998. Changing concentration, lifetime and climate forcing of atmospheric methane. *Tellus, Ser. B*, **50**, 128-150.
- Levin, I., Bergamaschi, P., Dorr, H. and Trapp, D. 1993. Stable Isotopic Signature of Methane from Major Sources in Germany. *Chemosphere*, **26**, 161-177.
- Levin, I., Glatzel-Mattheier, H., Marik, T., Cuntz, M., Schmidt, M. and Worthy, D. E. 1999. Verification of German methane emission inventories and their recent changes based on atmospheric observations. *J. Geophys. Res.*, **104**, 3447-3456.
- Liptay, K., Chanton, J., Czepiel, P. and Mosher, B. 1998. Use of stable isotopes to determine methane oxidation in landfill cover soils. *J. Geophys. Res.*, **103**, 8243-8250.
- Lowe, D. C., Brenninkmeijer, C. A. M., Brailsford, G. W., Lassey, K. R., Gomez, A. J. and Nisbet, E. G. 1994. Concentration and C-13 Records of Atmospheric Methane in New- Zealand and Antarctica - Evidence For Changes in Methane Sources. *J. Geophys. Res.*, **99**, 16913-16925.
- Lowe, D. C., Manning, M. R., Brailsford, G. W. and Bromley, A. M. 1997. The 1991-1992 atmospheric methane anomaly: Southern Hemisphere C-13 decrease and growth rate fluctuations. *Geophys. Res. Lett.*, **24**, 857-860.
- Lowry, D., Holmes, C. W., Rata, N. D., O'Brien, P. and Nisbet, E. G. 2001. London methane emissions: Use of diurnal changes in concentration and delta C-13 to identify urban sources and verify inventories. *J. Geophys. Res.*, **106**, 7427-7448.
- Miller, J. B. 1999 In *Department of Chemistry* University of Colorado, Boulder, pp. 162.

- Miller, J. B., Mack, K. A., Dissly, R., White, J. W. C., Dlugokencky, E. J. and Tans, P. P. 2002. Development of analytical methods and measurements of $^{13}\text{C}/^{12}\text{C}$ in atmospheric CH_4 from the NOAA/CMDL global air sampling network. *J. Geophys. Res.*, **In Press**.
- Montzka, S. A., Spivakovsky, C. M., Butler, J. H., Elkins, J. W., Lock, L. T. and Mondeel, D. J. 2000. New Observational Constraints for Atmospheric Hydroxyl on Global and Hemispheric Scales. *Science*, **288**, 500-503.
- Nakazawa, T., Machida, T., Tanaka, M., Fujii, Y., Aoki, S. and Watanabe, O. 1993. Differences of the Atmospheric CH_4 Concentration Between the Arctic and Antarctic Regions in Pre-Industrial/Pre-Agricultural Era. *Geophys. Res. Lett.*, **20**, 943-946.
- Olivier, J. G. J., Bouwman, A. F., Berdowski, J. J. M., C., V., Bloos, J. P. J., Visschedijk, A. H. J., van de Maas, C. W. M. and Zandveld, P. Y. J. 1999. Sectoral emission inventories of greenhouse gases for 1990 on per country basis as well as on 10 x 10. *Environ. Sci. Policy*, **2**, 241-264.
- Popp, T. J., Chanton, J. P., Whiting, G. J. and Grant, N. 1999. Methane stable isotope distribution at a Carex dominated fen in north central Alberta. *Global Biogeochem. Cycles*, **13**, 1063-1077.
- Prinn, R. G., Weiss, R. F., Miller, B. R., Huang, J., Alyea, F. N., Cunnold, D. M., Fraser, P. J., Hartley, D. E. and Simmonds, P. G. 1995. Atmospheric Trends and Lifetime of CH_3CCl_3 and Global OH Concentrations. *Science*, **269**, 187-192.

- Quay, P., Stutsman, J., Wilbur, D., Snover, A., Dlugokencky, E. and Brown, T. 1999. The isotopic composition of atmospheric methane. *Global Biogeochem. Cycles*, **13**, 445-461.
- Quay, P. D., King, S. L., Landsdown, J. M. and Wilbur, D. O. 1988. Isotopic composition of methane released from wetlands: implications for the increase in atmospheric methane. *Global Biogeochem. Cycles*, **2**, 385-397.
- Quay, P. D., King, S. L., Stutsman, J., Wilbur, D. O., Steele, L. P., Fung, I., Gammon, R. H., Brown, T. A., Farwell, G. W., Grootes, P. M. and Schmidt, F. H. 1991. Carbon isotopic composition of atmospheric CH₄: Fossil and biomass burning source strengths. *Global Biogeochem. Cycles*, **5**, 25-47.
- Randerson, J. T., Thompson, M. V., Conway, T. J., Fung, I. Y. and Field, C. B. 1997. The contribution of terrestrial sources and sinks to trends in the seasonal cycle of atmospheric carbon dioxide. *Global Biogeochem. Cycles*, **11**, 535-560.
- Rice, A. L., Gotoh, A. A., Ajie, H. O. and Tyler, S. C. 2001. High-precision continuous-flow measurement of delta C-13 and delta D of atmospheric CH₄. *Anal. Chem.*, **73**, 4104-4110.
- Ridgwell, A. J., Marshall, S. J. and Gregson, K. 1999. Consumption of atmospheric methane by soils: A process-based model. *Global Biogeochem. Cycles*, **13**, 59-70.
- Sansone, F. J., Popp, B. N., Gasc, A., Graham, A. W. and Rust, T. M. 2001. Highly elevated methane in the eastern tropical North Pacific and associated isotopically enriched fluxes to the atmosphere. *Geophys. Res. Lett.*, **28**, 4567-4570.

- Saueressig, G., Bergamaschi, P., Crowley, J. N., Fischer, H. and Harris, G. W. 1995. Carbon Kinetic Isotope Effect in the Reaction of CH₄ With Cl Atoms. *Geophys. Res. Lett.*, **22**, 1225-1228.
- Saueressig, G., Crowley, J. N., Bergamaschi, P., Bruhl, C., Brenninkmeijer, C. A. M. and Fischer, H. 2001. Carbon 13 and D kinetic isotope effects in the reactions of CH₄ with O(D-1) and OH: New laboratory measurements and their implications for the isotopic composition of stratospheric methane. *J. Geophys. Res.*, **106**, 23127-23138.
- Schoell, M. 1980. The hydrogen and carbon isotopic composition of methane from natural gases of various origins. *Geochim. Cosmochim. Acta*, **44**, 649-661.
- Singh, H. B., Thakur, A. N., Chen, Y. E. and Kanakidou, M. 1996. Tetrachloroethylene as an indicator of low Cl atom concentrations in the troposphere (vol 23, pg 1529, 1996). *Geophys. Res. Lett.*, **23**, 2713-2713.
- Smith, L. K., Lewis, W. M., Chanton, J. P., Cronin, G. and Hamilton, S. K. 2000. Methane emissions from the Orinoco River floodplain, Venezuela. *Biogeochemistry*, **51**, 113-140.
- Sowers, T. A. 2000a. The delta13C of Atmospheric CH₄ over the last 200 years as recorded in the GISP II ice core. *Eos Trans. AGU*, **81**, S20.
- Sowers, T. A. 2000b. The delta13C of atmospheric CH₄ over the past 30,000 years as recorded in the Taylor Dome ice core. *Eos Trans. AGU*, **81**, F78.
- Steele, L. P., Fraser, P. J., Rasmussen, R. A., Khalil, M. A. K., Conway, T. J., Crawford, A. J., Gammon, R. H., Masarie, K. A. and Thoning, K. W. 1987. The Global Distribution of Methane in the Troposphere. *J. Atmos. Chem.*, **5**, 125-171.

- Stevens, C. M. 1993 In *Atmospheric Methane: Sources, Sinks and Role in Global Change*(Ed, Khalil, M. A. K.) Springer-Verlag, Berlin, 11-21.
- Stevens, C. M. 1995. Carbon-13 isotopic abundance and concentration of atmospheric methane for background air in the southern and northern hemispheres from 1978 to 1989. **Publication 4388**.
- Stevens, C. M. and Rust, F. E. 1982. The Carbon Isotopic Composition of Atmospheric Methane. *J. Geophys. Res.*, **87**, 4879-4882.
- Tans, P. P. 1997. A note on isotopic ratios and the global atmospheric methane budget. *Global Biogeochem. Cycles*, **11**, 77-81.
- Tans, P. P., Fung, I. Y. and Takahashi, T. 1990. Observational Constraints On the Global Atmospheric Co₂ Budget. *Science*, **247**, 1431-1438.
- Thompson, A. M. 1992. The oxidizing capacity of the earth's atmosphere: probable past and future changes. *Science*, **256**, 1157-1165.
- Tyler, S. C. 1986. Stable Carbon Isotope Ratios in Atmospheric Methane and Some of its Sources. *J. Geophys. Res.*, **91**, 13,332-12,338.
- Tyler, S. C., Ajie, H. O., Gupta, M. L., Cicerone, R. J., Blake, D. R. and Dlugokencky, E. J. 1999. Stable carbon isotopic composition of atmospheric methane: A comparison of surface level and free tropospheric air. *J. Geophys. Res.*, **104**, 13895-13910.
- Tyler, S. C., Brailsford, G. W., Yagi, K., Minami, K. and Cicerone, R. J. 1994. Seasonal-Variations in Methane Flux and Delta(CH₄)C-13 Values for Rice Paddies in Japan and Their Implications. *Global Biogeochem. Cycles*, **8**, 1-12.

- Vaghjiani, G. L. and Ravishankara, A. R. 1991. New Measurement of the Rate Coefficient For the Reaction of Oh With Methane. *Nature*, **350**, 406-409.
- van Aardenne, J. A., Dentener, F. J., Olivier, J. G. J., Goldewijk, C. and Lelieveld, J. 2001. A 1 degrees x 1 degrees resolution data set of historical anthropogenic trace gas emissions for the period 1890-1990. *Global Biogeochem. Cycles*, **15**, 909-928.
- Vogt, R., Crutzen, P. J. and Sander, R. 1996. A mechanism for halogen release from sea-salt aerosol in the remote marine boundary layer. *Nature*, **383**, 327-330.
- Waldron, S., Lansdown, J. M., Scott, E. M., Fallick, A. E. and Hall, A. J. 1999. The global influence of the hydrogen isotope composition of water on that of bacteriogenic methane from shallow freshwater environments. *Geochim. Cosmochim. Acta*, **63**, 2237-2245.
- Walter, B. P. and Heimann, M. 2000. A process-based, climate-sensitive model to derive methane emissions from natural wetlands: Application to five wetland sites, sensitivity to model parameters, and climate. *Global Biogeochem. Cycles*, **14**, 745-765.
- Wingenter, O. W., Blake, D. R., Blake, N. J., Sive, B. C., Rowland, F. S., Atlas, E. and Flocke, F. 1999. Tropospheric hydroxyl radical and atomic chlorine concentrations, and mixing timescales determined from hydrocarbon and halocarbon measurements made over the Southern Ocean. *J. Geophys. Res.*, **104**, 21,819-21,828.

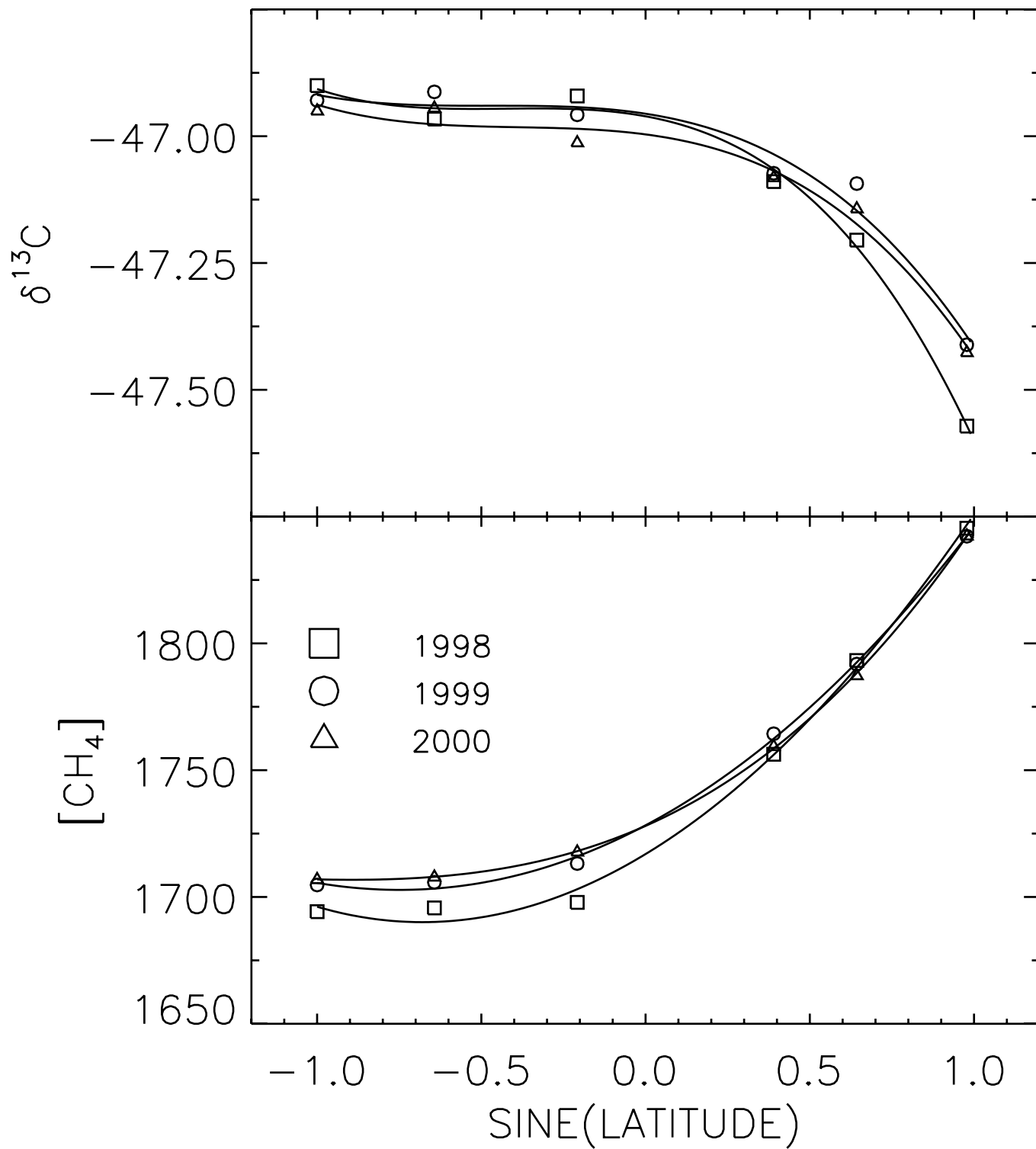


Figure 1

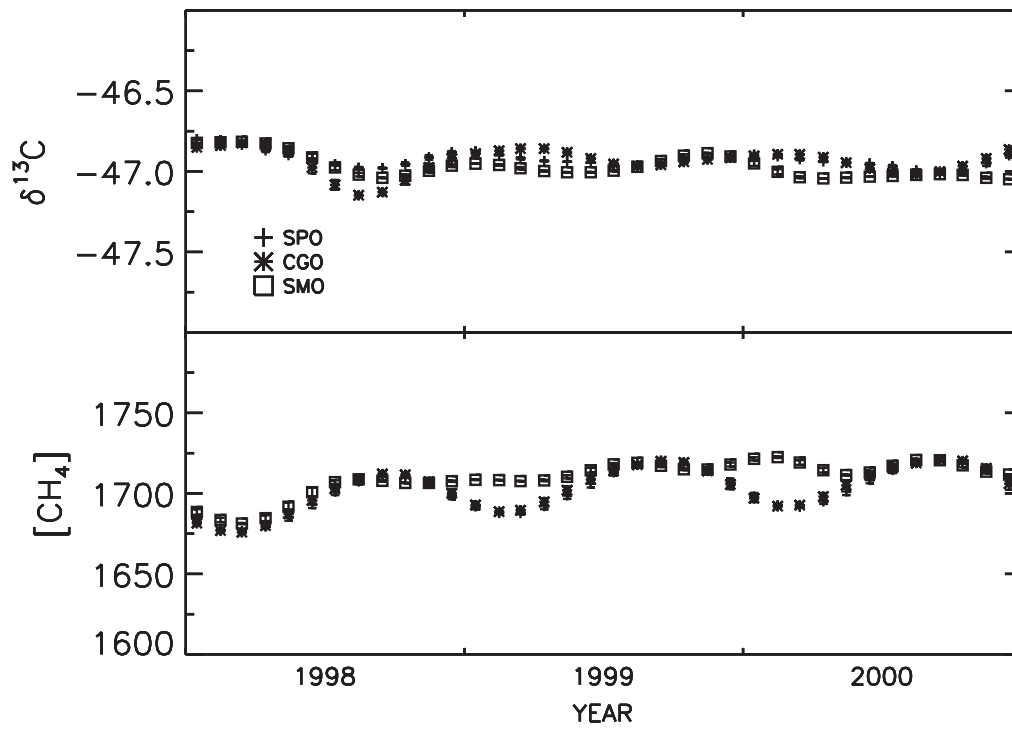
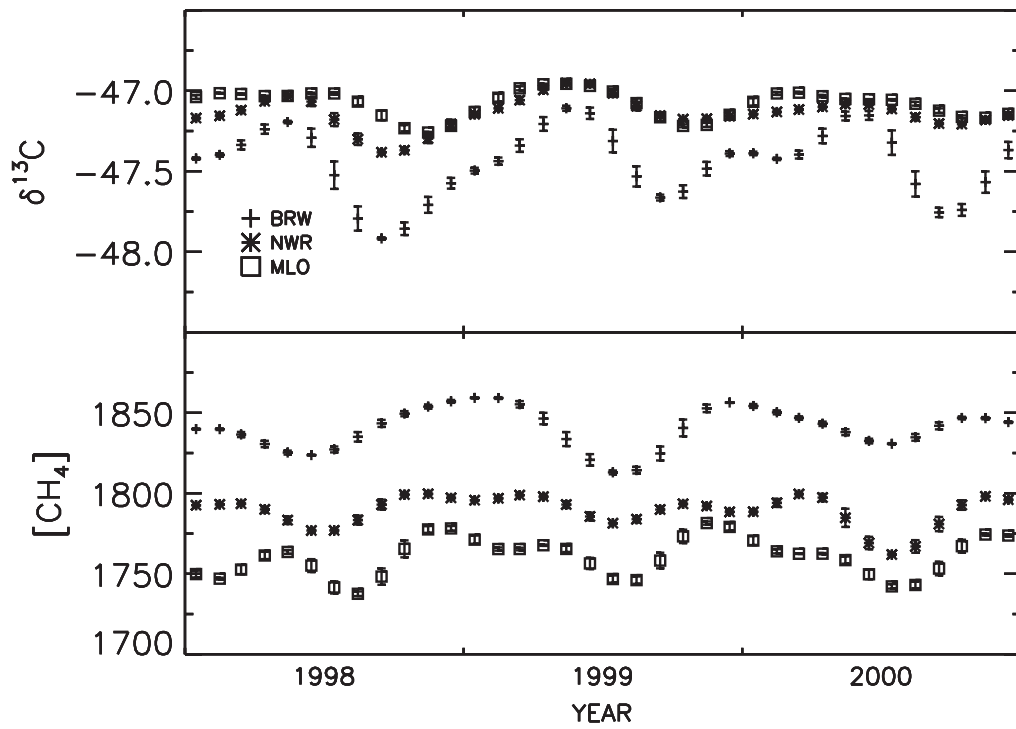


Figure 2

Figure 1.

Latitudinal gradient of CH₄ and δ¹³C during 1998-2000. The gradient is constructed from six NOAA/CMDL sites: (from north to south) Barrow, Alaska 71°N (BRW), Niwot Ridge, Colorado 40°N (NWR), Mauna Loa, Hawaii 20°N (MLO), American Samoa 14°S (SMO), Cape Grim, Tasmania 41°S (CGO), South Pole 90°S (SPO). The symbols are annual mean δ¹³C and CH₄ values at each station and the lines are cubic polynomial fits to the annual means. The latitude axis is scaled by sine of latitude to account for the reduction in zonal area with increasing latitude.

Figure 2.

Monthly mean seasonal cycles of CH₄ and δ¹³C from 1998-2000 at six NOAA/CMDL stations. The monthly means are calculated by sampling a curve fit to the raw data. This method accounts for missing data in some months at certain sites. The error bars are the standard deviations of sampled data used to construct the monthly mean and are not related to measurement precision. Station codes are identified in the text and in the caption for Figure 1.